

# Formal Verification of Deep Neural Networks for Object Detection

Yizhak Y. Elboher<sup>1\*</sup>, Avraham Raviv<sup>2\*</sup>, Yael Leibovich Weiss<sup>2</sup>, Omer Cohen<sup>2</sup>,  
Roy Assa<sup>2</sup>, Guy Katz<sup>1</sup>, and Hillel Kugler<sup>2</sup>

<sup>1</sup> The Hebrew University of Jerusalem, {yizhak.elboher,  
g.katz}@mail.huji.ac.il

<sup>2</sup> Bar-Ilan University, {ravivav1, roy.assa, leibovya, cohenomc,  
hillelk}@biu.ac.il

**Abstract.** Deep neural networks (DNNs) are widely used in real-world applications, yet they remain vulnerable to errors and adversarial attacks. Formal verification offers a systematic approach to identify and mitigate these vulnerabilities, enhancing model robustness and reliability. While most existing verification methods focus on image classification models, this work extends formal verification to the more complex domain of *object detection* models. We propose a formulation for verifying the robustness of such models and demonstrate how state-of-the-art verification tools, originally developed for classification, can be adapted for this purpose. Our experiments, conducted on various datasets and networks, highlight the ability of formal verification to uncover vulnerabilities in object detection models, underscoring the need to extend verification efforts to this domain. This work lays the foundation for further research into formal verification across a broader range of computer vision applications.

**Keywords:** Object Detection, Neural Networks, Formal Verification, Adversarial Attacks

## 1 Introduction

Deep neural networks (DNNs) have demonstrated remarkable capabilities [36], consistently achieving state-of-the-art performance across a wide range of domains such as computer vision (CV) [18, 36], natural language processing (NLP) [10, 17, 54], audio [6, 27] and video [5, 41]. Despite this significant success, the integration of DNNs in safety-critical industries like autonomous vehicles, aviation, financial services, and healthcare is very limited: their statistical nature makes them vulnerable to both innocent and malicious alterations, such that even small, often imperceptible perturbations to the input can lead to critical errors.

This vulnerability of DNNs has spawned an entire branch of research dedicated to their attack and defense. A key family of defense methods is based on formally verifying DNNs [33, 39], in order to prove their robustness to attacks.

---

\* These authors contributed equally.

Initially, DNN verification focused primarily on classification networks [33, 60]; and since then, there has been a growing interest in extending these methods to other areas such as natural language processing [13], reinforcement learning [4, 7], and explainability [8]. Despite these advances, the application of formal verification to other essential computer vision tasks remains underexplored. Notably, object detection and segmentation, despite their critical roles in many applications, have not yet been extensively studied in the context of formal verification techniques.

**Our Contributions.** In this work, we begin to bridge this gap by systematically exploring attacks and validating DNN robustness for object detection. Towards this end, we:

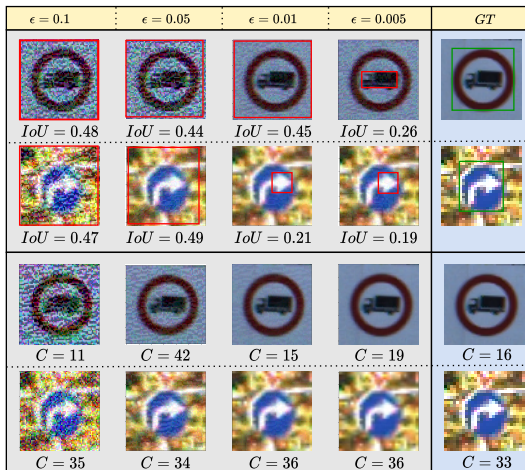
1. Cast various object detection attacks as formal verification problems. By establishing clear definitions, we set the stage for systematically assessing the robustness of models against various attacks.
2. Show how existing verification tools, primarily designed for classification tasks, can be adjusted to handle these new formulations. We develop an adaptation which offers practical insights into utilizing current tools to verify a broader range of computer vision tasks with minimal changes.
3. Implement our verification method and adapt a state-of-the-art verification tool to verify multiple object detection models on multiple datasets. Our code will be made publicly available upon paper acceptance.
4. Provide (i) examples of several attacks on object detectors, and (ii) robustness analysis of multiple object detection models and datasets; both demonstrate the need and importance of extending formal methods for DNNs to broader computer vision tasks.
5. Compare to other verification methods, which use Interval Bound Propagation (IBP), and demonstrate that our complete method is able to solve a significantly higher number of queries.

Figure 1 illustrates robustness threats (an object detector can fail in various ways) which were found by our method, highlighting the critical challenges our approach aims to address.

The rest of this paper is organized as follows. Sec. 2 provides an overview of related work on neural network verification and adversarial attacks in computer vision. Sec. 3 includes a general background on object detection and formal verification of DNNs. Sec. 4 outlines our methodology, presenting the formulation of several computer vision tasks as formal verification problems and detailing how verification tools can be adapted to handle these tasks. Sec. 5 presents our evaluation results on multiple models and datasets, demonstrating the effectiveness of our approach through examples. Finally, Sec. 6 summarizes our work and discusses future research directions.

## 2 Related Work

This work seeks to bridge the gap between object detection and formal verification of neural networks. State-of-the-art object detection methods, such as Faster



**Fig. 1.** Examples of attacked images. The rightmost column shows original images, while the others display attacked images with different noise levels (maximum allowed noise  $\epsilon$ ). The top two rows illustrate misdetection ( $IoU > 0.5$  is needed for correct detection, see Sec. 3), and the bottom two rows show misclassification into class  $C$  (class mapping is detailed in [56]).

R-CNN [49], YOLO [48], and SSD [40], leverage deep convolutional networks to deliver high accuracy and efficiency on diverse datasets. Besides common classification attacks [37], these models are also prone to patch-based attacks [50, 51] that involve adding adversarial patches to the image, and to adversarial camouflage [31, 61] which subtly alters the appearance of objects in order to make them “invisible” to the model. Such attacks highlight the importance of our work.

Our research builds upon the formal verification of deep neural networks. There are multiple verification approaches and tools, based on SMT solving [34, 57], symbolic interval propagation [28, 29], MILP and LP solving [12, 20, 26, 42, 53], and abstract interpretation [25, 45, 55, 60] with branch-and-bound mechanisms [11, 38, 43]. For our experiments here, we use the Alpha-Beta-CROWN verifier, which supports networks with multiple outputs and a variety of activation functions.

In addition to CV, formal verification of DNNs has been applied in NLP [13], reinforcement learning [1, 1, 35, 46, 47, 58], explainability [7, 8], generalization [2, 3], delta-debugging [24] and robustness assessment [21], and was extended in multiple directions, including proof production [32], abstraction [14, 23, 46, 59] and residual reasoning [22]. We believe these lines of work are complementary to ours, and it will be of interest to explore potential synergies between them in the future.

Most closely related to our work is the recent, independent and complementary work of Cohen et al. [15], in which the authors study the formal verification of DNN-based object detection models. While Cohen et al. define the underlying

verification problem in a manner similar to ours, the two approaches differ in the abstract domain used to encapsulate the IoU output. The work by Cohen et al. demonstrates the relevance of the line of work pursued in the present analysis, and the interest of large industrial corporations — Airbus, in this case — in the formal verification of object detection systems.

### 3 Preliminaries

In computer vision, various tasks require analyzing and interpreting visual data, each with its own unique challenges. In *image classification*, models categorize entire images into predefined classes. Formally, such a model  $f$  takes an input image  $m_0 \in \mathbb{R}^d$  and maps it to a class label  $c$ , chosen from a discrete set of possible labels  $\mathcal{C}$ :  $f(m_0) \in \mathcal{C}$ . Each label is assigned a confidence score, and the highest score indicates the predicted class.

*Object detection* (OD) extends image classification: it requires not only identifying the classes present in an image, but also localizing each object by predicting bounding boxes. An OD model takes an input image  $m$  and produces a set of bounding boxes  $\mathcal{B}$ . Each bounding box in  $\mathcal{B}$  is a tuple  $(x, y, h, w, c)$ , where  $(x, y)$  represents the coordinates of the top-left corner,  $(h, w)$  denotes its dimensions, and  $c$  signifies the detected object’s class label.

Given that perfect matching is rarely attainable, the comparison between actual prediction and the ground truth is assessed by calculating the *intersection over union* (IoU), which is the ratio between the intersection and union of the respective bounding boxes. If the IoU is above a predefined threshold  $\tau$  and the class is correct, the prediction is considered accurate.

An *adversarial attack* involves intentionally altering an original data point  $m_0 \in \mathbb{R}^d$  into a different one,  $m \in \mathbb{R}^d$ , with  $m \neq m_0$ , so that the altered data is interpreted differently by the model, potentially leading to incorrect or unintended outputs.

In formal verification, the goal is to ensure that a neural network satisfies specific desired properties under all possible input scenarios within a defined input set. The input set  $\mathcal{I}$  is often constrained by conditions  $\mathcal{C}_{in}$ , which limit the values the inputs can take. For instance, for an input  $\mathbf{x} \in \mathbb{R}^d$ ,  $\mathcal{I}$  can be defined as all points  $\mathbf{x} \in \mathbb{R}^d$  such that the perturbation from a base input  $\mathbf{x}_0$  is within a specified range, i.e.,  $|\mathbf{x} - \mathbf{x}_0| \leq \delta$ , where  $\delta$  denotes the allowed perturbation magnitude. The model’s output  $\mathcal{O} = f(\mathbf{x}) : \mathbf{x} \in \mathcal{I}$  is then checked against a set of output constraints  $\mathcal{C}_{out}^{neg}$ , which typically specify the negation of the desired behavior  $\mathcal{C}_{out}$ . The goal of verification is to show that there are no inputs within the input set  $\mathcal{I}$  which satisfying  $\mathcal{C}_{in}$ , whose outputs  $\mathcal{O}$  satisfy  $\mathcal{C}_{out}^{neg}$ . This can be formalized as:

$$\neg \exists m \in \mathcal{C}_{in}, \quad f(m) \in \mathcal{C}_{out}^{neg}$$

This ensures that the neural network behaves correctly for all inputs that satisfy the given constraints, providing a robust guarantee of the model’s reliability.

In image classification, the verification task involves ensuring that the model correctly predicts the class label under variations in the input. The input con-

straints  $\mathcal{C}_{in}$  typically define permissible modifications to an image  $\mathbf{x}_0$ , forming a set  $\mathcal{I}$  of perturbed inputs, while the output constraints  $\mathcal{C}_{out}$  require that the predicted class label remains consistent across all inputs in  $\mathcal{I}$ . Verification techniques in computer vision have largely been focused on image classification tasks, where maintaining consistent classification outcomes despite allowable perturbations is key.

**Object Detection: Threat Model.** In this work, we focus on a threat model where the attacker can alter the input by adding small perturbations to a given image, has white-box access to the model, and an unlimited number of queries to the model. Unlike the classification domain, which typically revolves around a singular option — misclassification — object detection presents a broader range of potential attack vectors, including:

1. *Misdetetection* (bounding box false negatives). In this scenario, the aim is to manipulate the model into missing the detection of genuine objects.
2. *Misclassification* (classifier error). This attack vector mirrors classification adversarial attacks and involves deliberately causing OD models to both miss or incorrectly label detected objects. Note that misdetection is a special case of misclassification.
3. *Overdetection* (bounding box false positives). The goal of this attack is fooling the network to detect objects that are not present in the image.

## 4 Object Detection Robustness as a Formal Verification Problem

In order to phrase robustness with respect to different attacks as formal verification queries, we need to formulate suitable input and output constraints  $P$  and  $Q$ , which express that the attack cannot occur. Then, by proving that  $P \Rightarrow Q$ , we prove that the attack is impossible; otherwise, we prove that the attack is feasible, and the satisfying assignment returned by the verifier constitutes an adversarial example. We begin by formally defining each attack vector in the threat model as a  $P \Rightarrow Q$  condition in Subsection 4.1; and then show how to translate these conditions into verification queries, with input and output constraints, in Subsection 4.2.

### 4.1 Formal Definition of Object Detection Attacks

For all the attacks above, since the threat model only permits a small perturbation on the original input, the input property should require small distance from the original input. Hence, the input constraint is defined as follows:

$$P := |x - x_0| < \epsilon$$

and limits the adversarial image to be sufficiently close to the original image.

For a given image, assume there are  $o_g$  ground truth tuples  $\{G_1, \dots, G_{o_g}\}$  in the image, each represented as a bounding box and class  $G_i = (x_i^g, y_i^g, h_i^g, w_i^g, c_i^g)$ ,

where  $x, y$  is the location,  $h$  is the height,  $w$  is the width, and  $c$  is the class. In addition, assume that the output of the OD model is represented as a set of  $o_d$  tuples  $\{D_1, D_2, \dots, D_{o_d}\}$ , where each  $D_j = (x_j^d, y_j^d, h_j^d, w_j^d, c_j^d)$  corresponds to an object which was detected by the model.

1. **Misdetetection:** The attack can occur when there exists a ground truth bounding box  $G_i$  which is not detected at all. Formally, when:

$$Q_1 := (o_g > o_d) \vee \left( \exists i \in [o_g] \forall j \in [o_d] : \text{IoU}(G_i, D_j) < \tau \right)$$

Therefore, the robustness of the model to misdetection is represented by  $P \Rightarrow \neg Q_1$ , where:

$$\neg Q_1 := (o_g \leq o_d) \wedge \left( \forall i \in [o_g] \exists j \in [o_d] : \text{IoU}(G_i, D_j) > \tau \right)$$

2. **Misclassification:** The attack can occur when there exists a ground truth object which is not classified correctly. It can be a result of either detection (the bounding box was not detected) or classification (correct bounding box with incorrect classification). Consequently, the attack is represented by

$$Q_2 := (o_g > o_d) \vee \left( \exists i \in [o_g] \forall j \in [o_d] : (\text{IoU}(G_i, D_j) < \tau) \vee (c_i^g \neq c_j^d) \right)$$

Therefore, the robustness of the model to misdetection is represented by  $P \Rightarrow \neg Q_2$ , where:

$$\neg Q_2 := (o_g \leq o_d) \wedge \left( \forall i \in [o_g] \exists j \in [o_d] : (\text{IoU}(G_i, D_j) > \tau) \wedge (c_i^g = c_j^d) \right)$$

3. **Overdetection:** To refute the robustness of the model to overdetection attacks, a concrete input with a bounding box which does not exist in the ground truth should be found. This requirement is expressed as follows:

$$Q_3 := (o_d > o_g) \vee \left( \exists j \in [o_d] \forall i \in [o_g] : (\text{IoU}(D_j, G_i) < \tau) \vee (c_i^g \neq c_j^d) \right)$$

The input constraint remains as before, and the output constraint for overdetection robustness is thus

$$\neg Q_3 := (o_d \leq o_g) \wedge \left( \forall j \in [o_d] \exists i \in [o_g] : (\text{IoU}(D_j, G_i) > \tau) \wedge (c_i^g = c_j^d) \right)$$

Properties  $P \Rightarrow \neg Q_1$ ,  $P \Rightarrow \neg Q_2$  and  $P \Rightarrow \neg Q_3$  ensure the robustness of the object detector with respect to misdetection, misclassification and overdetection attacks, respectively. However, they are not defined on the output of the model; instead, these properties include constraints on the IoU, which is not calculated by the model at all. For the verification query to be well-defined, its output constraint must deal with values of existing neurons in the network.

As explained later in Subsection 4.3, we deal with the case where  $o_d = o_g = 1$ , hence we avoid checking the related conditions ( $o_g \leq o_d$  for misdetection/misclassification and  $o_d \leq o_g$  for overdetection).

## 4.2 Generating Equivalent Verification Queries

In order to generate a standard verification query for each attack, we change both the model and the output constraint; we convert each query  $(f, P, \neg Q_i)$  to a query  $(f'_i, P, \neg Q'_i)$  such that  $f'_i$  is an extended network with a neuron that represents the result of  $\neg Q_i$ . Accordingly,  $\neg Q'_i$  is an updated output constraint on this neuron whose result in  $f'_i$  is equivalent to  $\neg Q_i$  in  $f$ . We show that the queries are equivalent by construction.

**Modeling IoU-related Conditions with Neural Layers.** The core idea of our method is to extend the architecture of the given network, by adding layers that model an equivalent condition to  $\text{IoU} > \tau$ . Handling the value of the IoU in a single neuron is challenging since the value of IoU is a result of division of two variables (intersection and union are not known a-priori), and division is an operator not supported by most modern verifiers.

In order to overcome this problem, we use an equivalent condition which can be verified without explicitly calculating the value of the IoU. The encoding of the equivalent condition only includes subtraction and multiplication (with a-priori known scalar) operators, and hence can be encoded with neural layers.

We encode the equivalent condition by adding layers to the network after the original output layer (the original layers of the model are not changed). The added layers implement the calculation of both values  $A_I$  and  $A_U$  of intersection and union, respectively. After computing those values in two single neurons, an additional consecutive layer implements the logic of the equivalent condition; the resulting value is positive if and only if the original condition  $\text{IoU} > \tau$  holds.

By the end of this section, we explain in detail how to use neural layers in order to calculate the intersection and union values from the output of an object detection model and store them into a couple of neurons, and how to encode the equivalent condition using these neurons with one additional neural layer.

**Intersection and Union.** Given a couple of ground truth bounding box and predicted bounding box,  $B_{gt} = (x_g, y_g, h_g, w_g, c_g)$  and  $B_{dt} = (x_d, y_d, h_d, w_d, c_d)$ , the calculation of intersection and union values involves only *max*, *min*, *add* and *subtract* operations. The intersection between  $B_{gt}$  and  $B_{dt}$  is a rectangle  $R$  with the following coordinates:

$$\begin{aligned} x_{i1} &= \max(x_g, x_d) & x_{i2} &= \min(x_g + w_g, x_d + w_d) \\ y_{i1} &= \max(y_g, y_d) & y_{i2} &= \min(y_g + h_g, y_d + h_d) \end{aligned}$$

The width ( $w_i$ ) and height ( $h_i$ ) of  $R$ , and the implied area of the intersection, denoted by  $A_I$ , are given by:

$$w_i = \max(0, x_{i2} - x_{i1}) \quad h_i = \max(0, y_{i2} - y_{i1}) \quad A_I = w_i \cdot h_i$$

The areas of the ground truth bounding box ( $A_g$ ) and the predicted bounding box ( $A_d$ ), as well as the implied area of the union ( $A_U$ ) are given by:

$$A_g = w_g \cdot h_g \quad A_d = w_d \cdot h_d \quad A_U = A_g + A_d - A_I$$

**IoU and Equivalent Constraint.** The IoU is defined as:

$$\text{IoU} = \frac{A_I}{A_U}$$

We should handle the IoU constraint which appears in misdetection, misclassification and overdetecion:  $\text{IoU} > \tau$ . We represent this constraint with an equivalent linear constraint, which can be easily encoded with neural layers:

$$\text{IoU} > \tau \Leftrightarrow \frac{A_I}{A_U} > \tau \Leftrightarrow A_I > \tau \cdot A_U \Leftrightarrow A_I - \tau \cdot A_U > 0$$

Fig. 2 illustrates how the IoU between a single ground truth bounding box and a single predicted bounding box can be encoded with neural layers. From now on, we denote with  $z$  the variable whose result is positive if and only if the condition  $\text{IoU} > \tau$  holds.

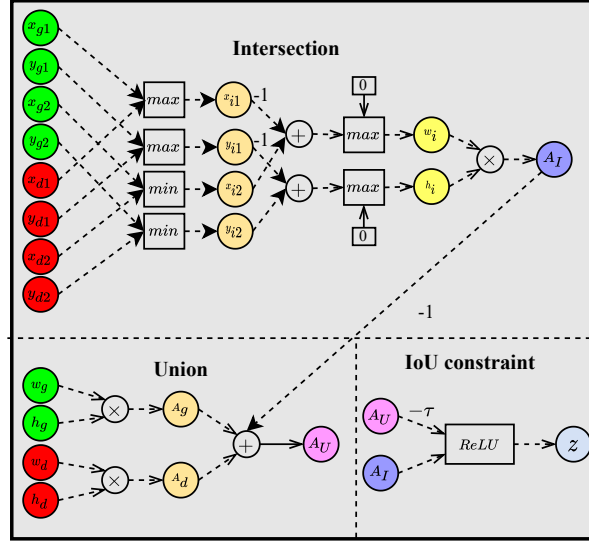


**Fig. 2.** Encoding IoU operation; At first, the area of the intersection and the area of the union are extracted into couple of neurons. Then, the equivalent condition is encoded using a single neural layer, and the output  $z$  is positive if and only if  $\text{IoU} > \tau$ .

#### 4.3 Redefining the Attacks

We now return to the attacks discussed above and show their full encoding as verification problems. Note: Since multi-object detection typically involves post-processing steps to reduce false positives, which are not formalized in this work, we focus on the single-object detection case. The extension to multi-object detection will be addressed in future work.



**Misdetetection.** This is the simplest case, where the output condition is simply  $\text{IoU} > \tau$ . In order to adapt the output constraint to the new network with equivalent constraint, we simply set  $z > 0$  as the new output constraint. The verification query is then  $(f', P, z > 0)$ .

**Misclassification.** The case of misclassification is more complex, where there are two conditions involved: (i)  $\text{IoU} < \tau$  and (ii)  $c_g = c_d$ . The first one is the same condition as in the misdetection case, whereas the second is the classic case of a local robustness query, which has been extensively explored. In order to combine both conditions without losing completeness, we present Algorithm 1. The algorithm implements a straightforward, anytime verification method, which checks both conditions for a limited time in each iteration, and increase the timeout if no result is obtained.

---

**Algorithm 1** Verify Robustness to Misclassification

---

**Input:** Object Detector  $f$ , initial timeout  $T > 0$

---

```

1: repeat
2:    $res_{det} = \text{verify-no-misdetection}(f, \text{IoU} > \tau, T)$ 
3:    $res_{clf} = \text{verify-equal-prediction}(f, c_g = c_d, T)$ 
4:   if  $res_{det} == \text{Safe} \ \& \ res_{clf} == \text{Safe}$  then
5:     return Safe
6:   else if  $res_{det} == \text{Unsafe}$  or  $res_{clf} == \text{Unsafe}$  then
7:     return Unsafe
8:   end if
9:    $T = 2 \cdot T$ 
10: until True

```

---

**Proposition 1.** *Alg. 1 preserves soundness and completeness.*

*Proof.* Alg. 1 runs a loop with increased time in each iteration. Given an underlying sound and complete verification tool, the times  $T_1, T_2$  it takes to the tool to solve each of the queries in lines 2,3 are finite (from its completeness). The loop in lines 1-10 eventually reach an iteration with timeout  $T > \max(T_1, T_2)$ , because the initial (positive) timeout is multiplied by 2 in the end of each iteration (line 9), and in this iteration answers from the underlying verification tool for both queries are obtained. As a result, at least one of the conditions in lines 4,6 must hold, and Alg. 1 finishes, hence its completeness.

When the algorithm returns an answer, it is *Unsafe* if at least one of the answers returned by the underlying sound verification tool is *Unsafe*, and it returns *Safe* only if both answers are *Safe*. Therefore, the final answer preserves the soundness of the underlying verification tool. ■

**Overdetection** In general, this scenario closely resembles the previous one. By temporarily swapping the roles of the ground-truth ( $G$ ) and predicted bounding

boxes ( $D$ ) in the definition of misclassification at Subsection 4.1, and applying the same verification process, we effectively check for over-detection. In the single object detection case, there is exactly one ground-truth bounding box, and exactly one predicted bounding box. In this case, over-detection is the same as misdetection; if one bounding box does not intersect with the other, then there are both the problem of missing a bounding box and the problem of detecting an incorrect box. As a result, no special adjustments are needed for this case, and the encoding for over-detection is the same as for misdetection.

## 5 Evaluation

To evaluate the effectiveness of our approach, we tested it on three different datasets. A brief overview of each is provided below.

1. *MNIST-OD*: This dataset is centered on digit detection and consists of images with a black background, where a single digit (0-9) from the widely used MNIST [16] dataset is randomly positioned within the frame.
2. *LARD (Large Aviation Recognition Dataset)*: This dataset consists of high-resolution aerial imagery, specifically curated for the task of detecting runways during aircraft approach and landing [19]. The variability in ground truth box sizes makes it a particularly challenging case for stability verification.
3. *GTSRB (German Traffic Sign Recognition Benchmark)*: This widely-used dataset for traffic sign recognition presents a realistic challenge for multi-class, single-image classification and detection, designed to test models under varying lighting conditions, perspectives, and distortions [30, 52].

Additional technical details for the three datasets are provided in Table 1.

**Table 1.** Dataset overview.

Dataset	Train Set Size	Test Set Size	Subject	#Classes	Image Size
LARD	100,000+	10,000+	Aircraft Taxiing	1	224×224
MNIST-OD	60,000	10,000	Digits Detection	10	90×90
GTSRB	39,209	12,630	Traffic Signs	43	64×64

For each dataset, we trained an object detector with the architecture proposed by Cohen et al. [15], which includes 2–3 convolutional layers followed by 2–3 linear layers; as well as two heads, one for detection and one for classification. The details of the models appear in Table 2.

To dispatch the verification queries, we used Alpha-Beta-CROWN [55], a state-of-the-art verification tool [9, 44]; although other verification tools could potentially be used as backends.

**Table 2.** Models Overview

Network	#Layers	#Parameters			Performance	
		Body	Classification head	Regression head	Class Accuracy	Mean IoU
LARD	5	16,887,104	516	-	-	0.52
MNIST-OD	6	1,985,200	2,570	1,028	98.4	0.864
GTSRB	6	1,985,200	2,570	11,051	83.2	0.732

### 5.1 Improving Alg. 1 by Customizing the Underlying Verifier

Alpha-Beta-CROWN tackles verification queries using three main techniques: (i) employing an adversarial attack to refute the property, (ii) utilizing incomplete verification techniques to prove the property, and (iii) applying complete verification by leveraging bounds obtained from the previous stages. This verification process in Alpha-Beta-CROWN is adapted to create Algorithm 2, an enhanced version of Algorithm 1, which separates the verification of misdetection and misclassification into distinct stages, prioritizing the most efficient methods early on. Initially (lines 2-6), attacks are applied to detect violations related to misdetection or misclassification. If a violation is found, *Unsafe* is returned. If both attacks fail, the verifier’s incomplete phase (lines 7-11) is applied to each query. If both queries are deemed *Safe*, the result is *Safe*. Otherwise, Algorithm 1 is executed with the remaining time, and its result is returned. Notice that  $attack(f, IoU > \tau)$  (line 3) and  $Safe\text{-incomplete}(f, IoU > \tau)$  (line 8) represent the attack and incomplete verification phases that are applied on the network after encoding the equivalent condition to  $IoU > \tau$ , as depicted in Fig. 4.2.

---

#### Algorithm 2 Verify No Misclassification: Improved Version

---

**Input:** Object Detector  $f$ , initial timeout  $T$

```

1: start = get_time()
2:  $res_{clf} = attack(f, c_g = c_d)$ 
3:  $res_{det} = attack(f, IoU > \tau)$ 
4: if ( $res_{det} = Unsafe$ ) or ( $res_{clf} = Unsafe$ ) then
5:   return Unsafe
6: end if
7:  $res_{clf} = Safe\text{-incomplete}(f, c_g = c_d)$ 
8:  $res_{det} = Safe\text{-incomplete}(f, IoU > \tau)$ 
9: if ( $res_{det} = Safe$ ) and ( $res_{clf} = Safe$ ) then
10:  return Safe
11: end if
12: return Algorithm 1( $f, T - (get\_time() - start)$ )

```

---

**Proposition 2.** *Algorithm 2 preserves soundness and completeness.*

*Proof.* Algorithm 2 adds preliminary steps to Algorithm 1. These steps are sound from the soundness of the underlying attack and *Safe-incomplete* stages of the

Alpha-Beta-CROWN, while the soundness of the final stage is derived from the soundness of Algorithm 1. Completeness is also derived from the completeness of Algorithm 1. ■

## 5.2 Results

We applied our method to assess each model’s robustness with respect to misdetection (which is equivalent to overdetection for single-object) and misclassification. We conducted our experiments on a wide range of 17 perturbation sizes for each image among the first 100 samples in each dataset, which sums up to 1700 total experiments for each dataset.

Fig. 3 shows the results for misdetection robustness (top), and the results for misclassification robustness (bottom). Green, yellow and red colors represent *Safe*, *Unknown* and *Unsafe* results, respectively. It can be seen that as epsilon (the maximal size of the perturbation) decreases, more robustness properties can be verified.

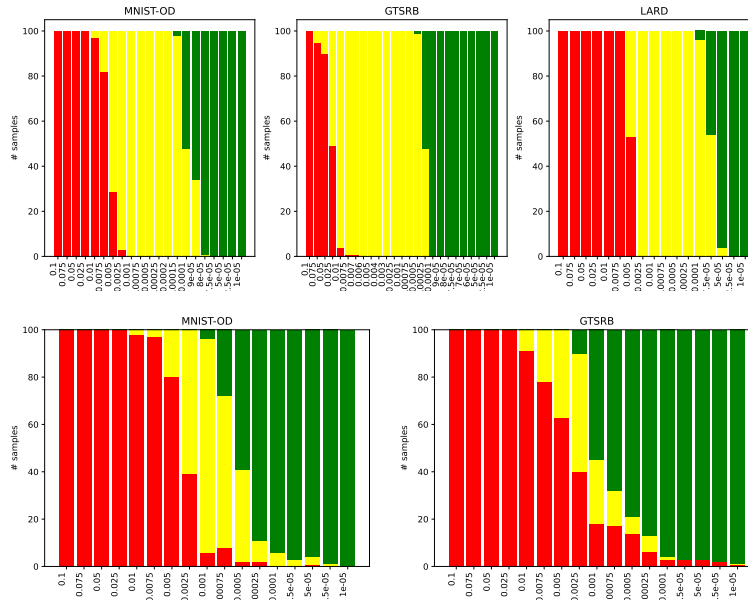


**Fig. 3.** (Top) Misdetection results per epsilon. (Bottom) Misclassification results per epsilon.

To measure runtime, we focused on the average runtime per sample. We tested the 5 smallest and 5 biggest epsilon values in Fig. 3 (bottom). in order to perform separated analysis for *Unsafe* and *Safe* instances. Among the 100 samples evaluated for each value, any experiments that exceeded a five-minutes time

limit were filtered out (less than 12% of the total samples). The average runtime per sample for *Unsafe* instances was 0.0052 seconds, while the average for *Safe* instances was 0.011 seconds. These results demonstrate that both refuting and certifying the robustness of the model to misdetection and misclassification are highly efficient, with fast execution times across both *Unsafe* and *Safe* instances.

### 5.3 Comparison to IBP-IoU

We compare the performance of our method to that introduced in [15], which employs interval bound propagation (IBP) for IoU computation in several configurations: Vanilla\_IoU, Optimal\_IoU, CROWN-IBP + Vanilla\_IoU, and CROWN-IBP + Optimal\_IoU. In the Vanilla\_IoU configuration, standard bounding of IoU operators is applied without interval propagation. The Optimal\_IoU configuration tightens these bounds for greater precision. Adding CROWN-IBP to each configuration contributes to yet greater precision.<sup>3</sup> The evaluation is conducted with a 5 minute timeout on the MNIST-OD and LARD datasets, focusing on average runtime and the number of *Safe*, *Unsafe*, and *Unknown* results.

As presented in Table 3, our method stands out as the only approach that successfully identifies *Unsafe* instances across both datasets. In addition, our method solves a total of 423 instances for MNIST-OD and 434 for LARD — about 70% more instances compared to the runner-up, which solves 240 instances for MNIST-OD and 263 for LARD.

In terms of runtime, our method is notably slower, with an average time of 2.73 seconds on MNIST-OD and 1.61 seconds on LARD, compared to fractions of a second for the other methods. However, this increase in computation time results in a more comprehensive verification, particularly in identifying unsafe scenarios, which are critical for robustness analysis.

In conclusion, while our method sacrifices some runtime efficiency, it offers a significant advantage by returning both *Safe* and *Unsafe* results, as well as greatly increasing the number of solved queries. This makes it a more reliable tool for verifying the robustness of neural networks.

**Table 3.** Comparison of verification methods on *MNIST-OD* and *LARD* datasets, showing the number of *Safe*, *Unsafe*, and *Unknown* results, along with average runtime.

Method	MNIST-OD				LARD			
	Safe	Unsafe	Unknown	Avg. Time (sec)	Safe	Unsafe	Unknown	Avg. Time (sec)
Vanilla_IoU	102	0	578	0.00010	61	0	659	0.00012
Optim_IoU	182	0	498	0.01143	90	0	630	0.01502
CROWN-IBP+Vanilla_IoU	207	0	473	0.00009	235	0	485	0.00009
CROWN-IBP+Optim_IoU	240	0	440	0.01099	263	0	457	0.01106
Ours	183	240	257	2.73072	135	259	286	1.60556

<sup>3</sup> Note that [15] also includes a version of CROWN without IBP, which uses CROWN to bound the output range without leveraging IBP’s interval propagation. However, this setting was not supported for the epsilon parameters we experimented with.

### 5.4 Qualitative Results

We provide further qualitative results in Figure 4. It illustrates multiple instances where our method identifies violation in misdetection robustness across different models, including high-resolution images. This occurs when the detected bounding boxes are either contained within, enclosing, or partially overlapping with the ground truth bounding box.

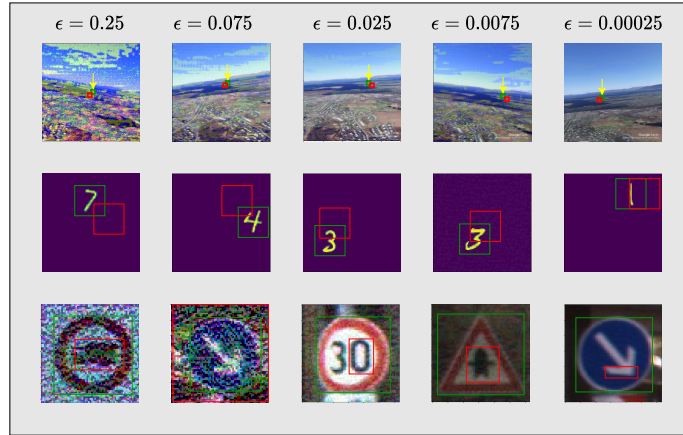


**Fig. 4. Misdetection examples on all datasets.** Ground truth (green bounding boxes), with misdetected objects (red bounding boxes) under adversarial attacks of varying noise levels.

### 5.5 Tau Effect

As mentioned earlier, all experiments initially used  $\tau = 0.5$ , a common assumption in object detection. In this section, we explore the impact of increasing  $\tau$  on the verification process. Figure 5 presents the results for two datasets, GT-SRB and MNIST-OD, under a misdetection attack. We evaluated three different values of  $\tau$  ( $\tau \in [0.5, 0.6, 0.7]$ ) and for each value we tested three corresponding  $\epsilon$  values:  $\epsilon \in \{10^{-2}, 10^{-3}, \dots\}$ . As illustrated, increasing the value of  $\tau$  results in a higher number of counterexamples and a reduction in the number of successfully verified samples. For instance, in the GTSRB dataset with  $\epsilon = 1e-2$ , the number of counterexamples rose from 4 to 28, and then to 58 as  $\tau$  increased from 0.5 to 0.6 and 0.7. Similarly, for  $\epsilon = 1e-4$ , the number of verified examples decreased from 100 to 84, and then to 55 with increasing  $\tau$ . These findings are consistent with expectations, as a higher  $\tau$  imposes stricter requirements on the model, making it easier to find vulnerabilities and more challenging to prove robustness.

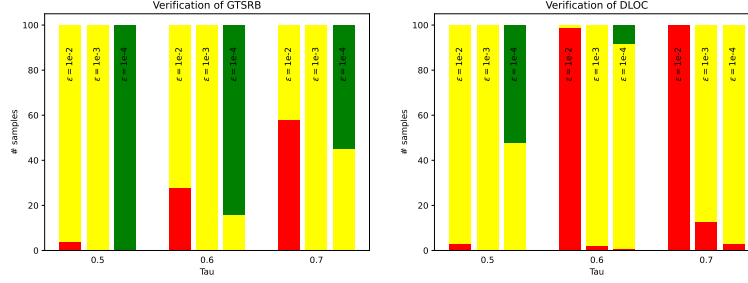


Fig. 5. Effect of  $\tau$ . The number of *Unsafe* results increases with  $\tau$ .

## 6 Conclusion

This work addresses the challenge of applying formal verification to ensure the safety of computer vision models, with a focus on extending its use from image classification to object detection. It introduces a framework to formalize multiple attack types — misdetection, misclassification, and overdetec-tion — by presenting them as formal verification problems for classification models. The study then outlines a method to apply verification using state-of-the-art tools to certify object detection models. The proposed approach is evaluated on various models and datasets, establishing a benchmark for future research.

The contribution of this work extends the formulation to new areas within the formal verification of DNNs, demonstrated through the implementation and examples presented. While further research is necessary, this work lays a strong foundation for integrating formal verification into computer vision, promising a safer future for these technologies.

## Acknowledgements

The research presented in this paper was (partially) funded by the The Israeli Smart Transportation Research Center (ISTRC).

## References

1. G. Amir, D. Corsi, R. Yerushalmi, L. Marzari, D. Harel, A. Farinelli, and G. Katz. Verifying Learning-Based Robotic Navigation Systems. In *Proc. 29th Int. Conf. on Tools and Algorithms for the Construction and Analysis of Systems (TACAS)*, pages 607–627, 2023.
2. G. Amir, O. Maayan, T. Zelazny, G. Katz, and M. Schapira. Verifying Generalization in Deep Learning. In *Proc. 35th Int. Conf. on Computer Aided Verification (CAV)*, pages 438–455, 2023.
3. G. Amir, O. Maayan, T. Zelazny, G. Katz, and M. Schapira. Verifying the Generalization of Deep Learning to Out-of-Distribution Domains. *Journal of Automated Reasoning (JAR)*, 68(3):17, 2024.

4. G. Amir, M. Schapira, and G. Katz. Towards Scalable Verification of Deep Reinforcement Learning. In *Proc. 21st Int. Conf. on Formal Methods in Computer-Aided Design (FMCAD)*, pages 193–203, 2021.
5. A. Arnab, M. Dehghani, G. Heigold, C. Sun, M. Lučić, and C. Schmid. VIVIT: A Video Vision Transformer. In *Proc. IEEE/CVF Int. Conf. on Computer Vision (ICCV)*, pages 6836–6846, 2021.
6. A. Baevski, Y. Zhou, A. Mohamed, and M. Auli. wav2vec 2.0: A Framework for Self-Supervised Learning of Speech Representations. In *Proc. Advances in Neural Information Processing Systems (NeurIPS)*, pages 12449–12460, 2020.
7. S. Bassan, G. Amir, D. Corsi, I. Refaeli, and G. Katz. Formally Explaining Neural Networks within Reactive Systems. In *Proc. 23rd Int. Conf. on Formal Methods in Computer-Aided Design (FMCAD)*, pages 10–22, 2023.
8. S. Bassan and G. Katz. Towards Formal XAI: Formally Approximate Minimal Explanations of Neural Networks. In *Proc. 29th Int. Conf. on Tools and Algorithms for the Construction and Analysis of Systems (TACAS)*, pages 187–207, 2023.
9. C. Brix, S. Bak, C. Liu, and T. T. Johnson. The Fourth Int. Verification of Neural Networks Competition (VNN-COMP 2023): Summary and Results, 2023. Technical Report. <http://arxiv.org/abs/2312.16760>.
10. T. B. Brown, B. Mann, N. Ryder, M. Subbiah, J. Kaplan, P. Dhariwal, A. Nee-lakantan, P. Shyam, G. Sastry, A. Askell, S. Agarwal, A. Herbert-Voss, G. Krueger, T. Henighan, R. Child, A. Ramesh, D. M. Ziegler, J. Wu, C. Winter, C. Hesse, M. Chen, E. Sigler, M. Litwin, S. Gray, B. Chess, J. Clark, C. Berner, S. McCandlish, A. Radford, I. Sutskever, and D. Amodei. Language Models are Few-Shot Learners, 2020. Technical Report. <http://arxiv.org/abs/2005.14165>.
11. R. Bunel, J. Lu, I. Turkaslan, P. H. Torr, P. Kohli, and M. P. Kumar. Branch and Bound for Piecewise Linear Neural Network Verification. *Journal of Machine Learning Research*, 21(42):1–39, 2020.
12. R. R. Bunel, I. Turkaslan, P. Torr, P. Kohli, and P. K. Mudigonda. A Unified View of Piecewise Linear Neural Network Verification. In *Proc. Advances in Neural Information Processing Systems (NeurIPS)*, 2018.
13. M. Casadio, T. Dinkar, E. Komendantskaya, L. Arnaboldi, O. Isac, M. L. Dag-gitt, G. Katz, V. Rieser, and O. Lemon. NLP Verification: Towards a General Methodology for Certifying Robustness, 2024. Technical Report. <http://arxiv.org/abs/2403.10144>.
14. E. Cohen, Y. Y. Elboher, C. Barrett, and G. Katz. Tighter Abstract Queries in Neural Network Verification. In *Proc. 24th Int. Conf. on Logic for Programming, Artificial Intelligence and Reasoning (LPAR)*, volume 94, pages 124–143, 2023.
15. N. Cohen, M. Ducoffe, R. Boumazouza, C. Gabreau, C. Pagetti, X. Pucel, and A. Galametz. Verification for Object Detection – IBP IoU, 2024. Technical Report. <http://arxiv.org/abs/2403.08788>.
16. L. Deng. The MNIST Database of Handwritten Digit Images for Machine Learning Research. *IEEE Signal Processing Magazine*, 29(6):141–142, 2012.
17. J. Devlin, M.-W. Chang, K. Lee, and K. Toutanova. BERT: Pre-training of Deep Bidirectional Transformers for Language Understanding, 2019. Technical Report. <http://arxiv.org/abs/1810.04805>.
18. A. Dosovitskiy, L. Beyer, A. Kolesnikov, D. Weissenborn, X. Zhai, T. Unterthiner, M. Dehghani, M. Minderer, G. Heigold, S. Gelly, J. Uszkoreit, and N. Houlsby. An Image is Worth 16x16 Words: Transformers for Image Recognition at Scale, 2021. Technical Report. <http://arxiv.org/abs/2010.11929>.



19. M. Ducoffe, M. Carrere, L. Féliers, A. Gauffriau, V. Mussot, C. Pagetti, and T. Sammour. LARD—Landing Approach Runway Detection—Dataset for Vision Based Landing, 2023. Technical Report. <http://arxiv.org/abs/2304.09938>.
20. S. Dutta, S. Jha, S. Sanakaranarayanan, and A. Tiwari. Output Range Analysis for Deep Neural Networks, 2017. Technical Report. <http://arxiv.org/abs/1709.09130>.
21. Y. Elboher, R. Elsaleh, O. Isac, M. Ducoffe, A. Galametz, G. Povéda, R. Boumazouza, N. Cohen, and G. Katz. Robustness Assessment of a Runway Object Classifier for Safe Aircraft Taxiing. In *Proc. 43rd Digital Avionics Systems Conf. (DASC)*, 2024.
22. Y. Y. Elboher, E. Cohen, and G. Katz. Neural Network Verification using Residual Reasoning. In *Int. Conf. on Software Engineering and Formal Methods (SEFM)*, pages 173–189, 2022.
23. Y. Y. Elboher, J. Gottschlich, and G. Katz. An Abstraction-Based Framework for Neural Network Verification. In *Proc. 32th Int. Conf. on Computer Aided Verification (CAV)*, pages 43–65, 2020.
24. R. Elsaleh and G. Katz. DelBugV: Delta-Debugging Neural Network Verifiers. In *Proc. 23rd Int. Conf. on Formal Methods in Computer-Aided Design (FMCAD)*, pages 34–43, 2023.
25. C. Ferrari, M. N. Müller, N. Jovanovic, and M. Vechev. Complete Verification via Multi-Neuron Relaxation Guided Branch-and-Bound, 2022. Technical Report. <http://arxiv.org/abs/2205.00263>.
26. M. Fischetti and J. Jo. Deep Neural Networks and Mixed Integer Linear Optimization. *Constraints*, 23(3):296–309, 2018.
27. A. Gulati, J. Qin, C.-C. Chiu, N. Parmar, Y. Zhang, J. Yu, W. Han, S. Wang, Z. Zhang, Y. Wu, and R. Pang. Conformer: Convolution-augmented Transformer for Speech Recognition, 2020. Technical Report. <http://arxiv.org/abs/2005.08100>.
28. P. Henriksen and A. Lomuscio. Efficient Neural Network Verification via Adaptive Refinement and Adversarial Search. In *Proc. European Conf. on Artificial Intelligence (ECAI)*, 2020.
29. P. Henriksen and A. Lomuscio. DEEPSPLIT: An Efficient Splitting Method for Neural Network Verification via Indirect Effect Analysis. In *Proc. 30th Int. Joint Conf. on Artificial Intelligence (IJCAI)*, pages 2549–2555, 2021.
30. S. Houben, J. Stallkamp, J. Salmen, M. Schlipsing, and C. Igel. Detection of Traffic Signs in Real-World Images: The German Traffic Sign Detection Benchmark. In *Proc. Int. Joint Conf. on Neural Networks (IJCNN)*, pages 1–8, 2013.
31. L. Huang, C. Gao, Y. Zhou, C. Xie, A. L. Yuille, C. Zou, and N. Liu. Universal Physical Camouflage Attacks on Object Detectors. In *Proc. IEEE/CVF Conf. on Computer Vision and Pattern Recognition (CVPR)*, pages 720–729, 2020.
32. O. Isac, C. W. Barrett, M. Zhang, and G. Katz. Neural Network Verification with Proof Production. In *Proc. 22nd Int. Conf. on Formal Methods in Computer-Aided Design (FMCAD)*, pages 38–48, 2022.
33. G. Katz, C. Barrett, D. L. Dill, and K. Julian. Reluplex: An Efficient SMT Solver for Verifying Deep Neural Networks. In *Proc. 29th Int. Conf. on Computer Aided Verification (CAV)*, pages 97–117, 2017.
34. G. Katz, D. A. Huang, D. Ibeling, K. Julian, C. Lazarus, R. Lim, P. Shah, S. Thakoor, H. Wu, A. Zeljic, D. L. Dill, M. J. Kochenderfer, and C. Barrett. The Marabou Framework for Verification and Analysis of Deep Neural Networks. In *Proc. 31th Int. Conf. on Computer Aided Verification (CAV)*, pages 443–452, 2019.

35. Y. Kazak, C. Barrett, G. Katz, and M. Schapira. Verifying Deep-RL-Driven Systems. In *Proc. Workshop on Network Meets AI & ML (NetAI)*, pages 83–89, 2019.
36. A. Krizhevsky, I. Sutskever, and G. E. Hinton. ImageNet Classification with Deep Convolutional Neural Networks. In *Proc. Advances in Neural Information Processing Systems (NeurIPS)*, 2012.
37. A. Kurakin, I. J. Goodfellow, and S. Bengio. Adversarial Machine Learning at Scale. In *Proc. Int. Conf. on Learning Representations (ICLR)*, 2017.
38. A. H. Land and A. G. Doig. An Automatic Method of Solving Discrete Programming Problems. *Econometrica*, 28(3):497–520, 1960.
39. C. Liu, T. Arnon, C. Lazarus, C. Strong, C. Barrett, and M. J. Kochenderfer. Algorithms for Verifying Deep Neural Networks. *Foundations and Trends in Optimization*, 4(3-4):244–404, 2021.
40. W. Liu, D. Anguelov, D. Erhan, C. Szegedy, S. E. Reed, C.-Y. Fu, and A. C. Berg. SSD: Single Shot MultiBox Detector, 2015. Technical Report. <http://arxiv.org/abs/1512.02325>.
41. Z. Liu, J. Ning, Y. Cao, Y. Wei, Z. Zhang, S. Lin, and H. Hu. Video Swin Transformer. In *Proc. IEEE/CVF Conf. on Computer Vision and Pattern Recognition (CVPR)*, pages 3202–3211, 2022.
42. A. Lomuscio and L. Maganti. An Approach to Reachability Analysis for Feed-Forward ReLU Neural Networks, 2017. Technical Report. <http://arxiv.org/abs/1706.07351>.
43. D. R. Morrison, S. H. Jacobson, J. J. Sauppe, and E. C. Sewell. Branch-and-bound Algorithms: A Survey of Recent Advances in Searching, Branching, and Pruning. *Discrete Optimization*, 19:79–102, 2016.
44. M. N. Müller, C. Brix, S. Bak, C. Liu, and T. T. Johnson. The Third Int. Verification of Neural Networks Competition (VNN-COMP 2022): Summary and Results, 2023. Technical Report. <http://arxiv.org/abs/2212.10376>.
45. M. N. Müller, G. Makarchuk, G. Singh, M. Püschel, and M. Vechev. PRIMA: General and Precise Neural Network Certification via Scalable Convex Hull Approximations. *Proc. ACM on Programming Languages*, 6(POPL):1–33, jan 2022.
46. A. Raviv, E. Bronshtein, O. Reginiano, M. Aluf-Medina, and H. Kugler. Learning Through Imitation by Using Formal Verification. In *Proc. Int. Conf. on Current Trends in Theory and Practice of Computer Science (SOFSEM)*, pages 342–355, 2023.
47. A. Raviv, Y. Gerber, L. Benzinou, M. Aluf-Medina, and H. Kugler. Prediction and Control of Stochastic Agents Using Formal Methods. In *Proc. 6th Workshop on Formal Methods for ML-Enabled Autonomous Systems (FoMLAS)*, pages 29–34, 2023.
48. J. Redmon, S. Divvala, R. Girshick, and A. Farhadi. You Only Look Once: Unified, Real-Time Object Detection. In *Proc. IEEE Conf. on Computer Vision and Pattern Recognition (CVPR)*, pages 779–788, 2016.
49. S. Ren, K. He, R. B. Girshick, and J. Sun. Faster R-CNN: Towards Real-Time Object Detection with Region Proposal Networks. In *Proc. Advances in Neural Information Processing Systems (NeurIPS)*, pages 91–99, 2015.
50. A. Roy, M. Abadi, and J. Gilmer. Adversarial Patch. In *Proc. 31st Conf. on Neural Information Processing Systems (NeurIPS)*, 2017.
51. A. Sharma, Y. Bian, P. Munz, and A. Narayan. Adversarial patch attacks and defences in vision-based tasks: A survey, 2022. Technical Report. <http://arxiv.org/abs/2206.08304>.

52. J. Stallkamp, M. Schlipsing, J. Salmen, and C. Igel. The German Traffic Sign Recognition Benchmark: A Multi-Class Classification Competition. In *Proc. Int. Joint Conf. on Neural Networks (IJCNN)*, pages 1453–1460, 2011.
53. V. Tjeng, K. Xiao, and R. Tedrake. Evaluating Robustness of Neural Networks with Mixed Integer Programming, 2017. Technical Report. <http://arxiv.org/abs/1711.07356>.
54. A. Vaswani, N. Shazeer, N. Parmar, J. Uszkoreit, L. Jones, A. N. Gomez, L. Kaiser, and I. Polosukhin. Attention Is All You Need, 2023. Technical Report. <http://arxiv.org/abs/1706.03762>.
55. S. Wang, H. Zhang, K. Xu, X. Lin, S. Jana, C.-J. Hsieh, and Z. J. Kolter. Beta-CROWN: Efficient Bound Propagation with Per-Neuron Split Constraints for Complete and Incomplete Neural Network Verification. In *Proc. Advances in Neural Information Processing Systems (NeurIPS)*, 2021.
56. L. Wen and K.-H. Jo. Traffic Sign Recognition and Classification with Modified Residual Networks. In *Proc. IEEE/SICE Int. Symposium on System Integration (SSI)*, pages 835–840, 2017.
57. H. Wu, O. Isac, A. Zeljić, T. Tagomori, M. Daggitt, W. Kokke, I. Refaeli, G. Amir, K. Julian, S. Bassan, et al. Marabou 2.0: A Versatile Formal Analyzer of Neural Networks. In *Proc. 36th Int. Conf. on Computer Aided Verification (CAV)*, 2024.
58. R. Yerushalmi, G. Amir, A. Elyasaf, D. Harel, G. Katz, and A. Marron. Scenario-Assisted Deep Reinforcement Learning. In *Proc. 10th Int. Conf. on Model-Driven Engineering and Software Development (MODELSWARD)*, pages 310–319, 2022.
59. R. Yerushalmi, G. Amir, A. Elyasaf, D. Harel, G. Katz, and A. Marron. Enhancing Deep Reinforcement Learning with Scenario-Based Modeling. *SN Computer Science*, 4(2):156, 2023.
60. H. Zhang, T.-W. Weng, P.-Y. Chen, C.-J. Hsieh, and L. Daniel. Efficient Neural Network Robustness Certification with General Activation Functions. In *Proc. Advances in Neural Information Processing Systems (NeurIPS)*, 2018.
61. Y. Zhang, H. Foroosh, P. David, and B. Gong. CAMOU: Learning Physical Vehicle Camouflages to Adversarially Attack Detectors in the Wild. In *Proc. Int. Conf. on Learning Representations (ICLR)*, 2018.